Available online at www.sciencedirect.com

ScienceDirect

Procedia CIRP 14 (2014) 107 – 112

www.elsevier.com/locate/procedia

6th CIRP International Conference on High Performance Cutting, HPC2014

Dissolution of Iron-Chromium Carbides during White Layer Formation induced by Hard Turning of AISI 52100 Steel

S. B. Hosseini[a,]*, R. Dahlgren[a], K. Ryttberg[b], U. Klement[a]

[a]*Department of Materials and Manufacturing Technology, Chalmers University of Technology, Rännvägen 2A, Gothenburg SE-412 96, Sweden,*
[b]*AB SKF, Hornsgatan 1, Gothenburg SE-415 50, Sweden*

* Corresponding author. Tel.: +46-31-337-2854.E-mail address: seyed.b.hosseini@gmail.com

Abstract

The $(Fe, Cr)_3C$ carbide morphology in the surface region of hard turned bainitic AISI 52100 steel was investigated using both experimental techniques and simulations, where microstructural analysis was correlated with analytical studies of the carbide dissolution kinetics using DICTRA[1]. The experimental results showed that for both predominantly thermally and mechanically induced white layers no significant carbide dissolution took place down to a depth of 20 µm below the machined surfaces. This was confirmed by the analytical results from DICTRA, which showed that no significant carbide dissolution should take place during hard turning given the short contact times. Within the hard turned surfaces up to ~12% of the carbides were elongated, indicating plastic deformation of the carbides during machining.

Keywords: Carbide dissolution, DICTRA simulation, White layer, Hard turning, Surface integrity, AISI 52100 steel,

1. Introduction

Historically, grinding has been used as the final machining operation of hardened metallic materials because of high process robustness, small dimensional variations of the workpiece, good surface roughness quality, and generation of compressive residual stresses [1]. Over the last decades, the interest in hard turning has steadily increased. The process enables a high degree of flexibility, comparatively short setup times and environmental compatibility [2]. Also the development of Cubic-Boron-Nitride cutting tool materials and geometries has resulted in a more robust process. Hence, the hard turning process has become both a complementary and a replacing process to grinding. However, even though hard turning can produce comparable surface qualities to grinding, the process is still not widely accepted as the final machining operation in the manufacturing industry. As discussed by Bartarya and Choudhury [3], the major reasons are connected to the tool wear that results in the generation of tensile residual stresses, larger dimensional variations of the final component, and surface induced white layers. The formation mechanisms of white layers during hard turning have been extensively studied over the last decades [4-7]. For example, Chou and Evans [4] concluded that white layer formation in hard turning of AISI 52100 steel was mainly thermally activated and that the high temperatures reached in cutting caused reversed martensitic transformation. Given the short duration of contact between the tool and the workpiece material, the authors concluded that the time was too short to affect the $(Fe, Cr)_3C$ carbides in the microstructure. In contrast, Akcan et al. [5] and Zurecki et al. [6] concluded that the combination of high thermal energy input and intense plastic shearing in the material during hard turning resulted in a refined grain structure and nearly complete carbide dissolution in AISI 52100 steel. In comparison when using transmission electron microscopy, Barry and Byrne [7] observed diffuse and continuous diffraction rings for cementite carbides when analyzing hard turned induced white layers of BS 8170M40 and low alloyed tool steels, compared to the discrete spots as found in the unaffected microstructure.

[1]DICTRA is a trademark of ThermoCalc Software Inc., SE-113 47 Stockholm, Sweden.

Selection and peer-review under responsibility of the International Scientific Committee of the 6th CIRP International Conference on High Performance Cutting
doi:10.1016/j.procir.2014.03.095

Because of the transition from discrete spots to continuous rings, the authors concluded that the carbide morphology had been affected during white layer formation. They suggested that the carbide refinement could have occurred through complete dissolution and re-precipitation. Evidently, contradictory results have been reported and the presented microstructure constituents and mechanical properties have been of different nature for white layers generated at comparable machining conditions and for comparable materials.

The aim of the present study was to reveal the influence of hard turning on the $(Fe, Cr)_3C$ carbides in white layers generated in AISI 52100 steel. The carbides were characterized regarding their distribution, size, and shape (aspect ratio, a/b) before and after hard turning. The dissolution kinetics of the carbides were also analyzed with DICTRA[1], which is a diffusion-controlled transformation simulation tool based on multi-component diffusion and thermodynamic data. The analytical results were evaluated with respect to the experimental results.

2. Experimental

The hard turning tests were conducted on a bainitic hardened (60±1 HRC) AISI 52100 steel with carbon and chromium contents of 0.95 wt.% and 1.42 wt.%, respectively, and containing less than 1 vol.% of retained austenite. During machining, CBN inserts with chamfer land of 0.12 mm and an angle of -25° were used. The clearance angle and the nose radius were 7° and 0.8 mm respectively. The cutting parameters such as depth of cut, feed rate, tool wear and cutting speed were chosen according to previous investigations made by the authors [8]. The tool flank wear and the cutting speed were varied in a systematic way to create both predominantly thermally (T-WL) and mechanically (M-WL) induced white layers as proposed by Hosseini et al. [8]. During machining, water based cutting fluid containing 5% oil was applied on the rake side with a pressure of 5 bar. Imaging of the cross-sectional microstructure of the machined surfaces was performed in a LEO 1550 field emission gun scanning electron microscope (FEG-SEM) using an in-lens secondary electron detector and an accelerating voltage of 0.2 kV.

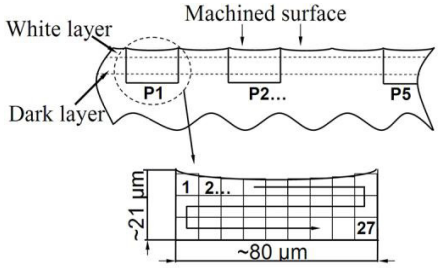

Fig. 1: P1 through P5 show the randomly selected areas chosen for carbide morphology analysis at the cross-section of a hard turned sample.

On each sample five areas sized 80x20 µm^2 were randomly selected, see P1 to P5 in Fig. 1, resulting in a total analyzed area of 400x20 µm^2. As shown in Fig. 1, each area was further divided into 27 segments of ~9x7 µm^2 in size, which resulted in 135 SEM images to be analyzed for each sample (~2500 carbides/sample). To study the carbide morphology in the unaffected microstructure, one of the samples was randomly selected and the carbides were analyzed at a depth of ~1 mm beneath the machined surface.

3. Simulation

DICTRA is as mentioned a tool for simulation of diffusion-controlled transformation, which is based on multicomponent diffusion using both thermodynamic and kinetic data [9]. During simulations, the databases TCFE6 and MOB1 were used to retrieve appropriate thermodynamic and mobility data. In the present study, the cell approach with a moving boundary model was used, which was defined in the ternary system containing iron, chromium and carbon (Fe-Cr-C). As shown in Fig. 2, the microstructure was simplified into a spherical cell structure containing the austenite (γ) phase and a single spherical carbide (θ) particle in the center of the cell. A system of three such cells was constructed with sizes and interparticle distances corresponding to the carbide morphology as observed in the machined samples. Cell coupling was achieved by requiring the activity of each component (Fe, Cr, C) at the common cell boundaries to be identical and the total amount of each component to be constant. To maintain the overall mass balance, the net diffusional fluxes of the elements between the cells was assumed to be zero ($\sum Ji = 0$), which was achieved by iteratively determining an activity resulting in a zero net sum of fluxes. The cell size was fixed during simulation, which means that the outer boundary of the cell was immobile and only the carbide/austenite interface was mobile [9].

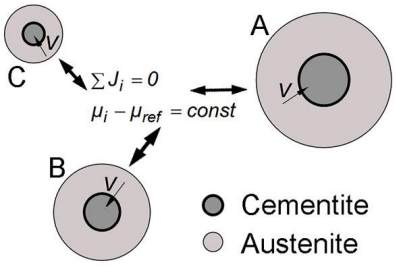

Fig. 2: Illustration of the design of the carbide system used in the DICTRA simulations. V indicated the direction of interface migration.

The boundary condition at the interface between the γ- and θ-phases was determined by the local equilibrium assumption as described by Ågren and Vassilev [10]. This assumption implies that the chemical potential is constant across the phase interface and the concentration of the components can be extracted from phase diagrams. The transformation rate is thus solely controlled by the diffusion of the components to and from the interface and effects such as curved interfaces and finite mobility of the interface as well as solute drag and elastic stresses are disregarded [11]. The contact times, temperatures and pressures corresponding to the hard turning parameters used in the present study have previously been investigated by the authors [12, 13] and are summarized in

Table 1. By using the information as input data for DICTRA, simulations could be run under realistic conditions. The simulations were carried out only for those machining conditions that resulted in predominantly thermally induced white layers where the cutting temperatures had been above the phase transformation temperature, A_{c1}, 750°C. The cell size was calculated according to equation 1 once the carbide volume fraction was experimentally determined.

$$r_{tot} = \frac{r_{(Fe,Cr)_3C}}{\sqrt[3]{V_{f\,(Fe,Cr)_3C}}} \qquad (1)$$

Here r_{tot} is the cell radius, $r_{(Fe, Cr)3C}$ is the radius of the carbides and $Vf_{(Fe, Cr)3C}$ is the carbide volume fraction. The distance between the carbides was set by the size of the γ-phase around the particles. Furthermore, the γ-phase was assumed to inherit the chemical composition of the prior structure (bainite), which was estimated to contain 0.7 wt.%- C and 1.0 wt.% Cr [8, 14]. The chromium content of the carbides was assumed to be 9.0 wt.% as reported by Beswick [14]. In Table 1, the final carbide diameters, cell diameters and the thickness of the austenitic regions for the three cells used in the simulations, A, B and C, are provided.

Table 1: The simulated machining conditions and constructed carbide morphologies used in DICTRA [12].

Simulation conditions	**Contact time, *t* [µs]**	**Temperature, *T* [°C]**	**Pressure, *p* [GPa]**
Tool/workpiece conditions	10 - 500	750 - 1000	0.0001, 1 - 4
Constructed carbide morphology	***θ*-diameter [µm]**	**Cell diameter [µm]**	**Thickness of γ-region [µm]**
A	0.50	1.4	0.45
B	0.25	0.7	0.23
C	0.20	0.36	0.18

4. Results and discussions

Fig. 3 shows a light optical and an SEM image of the cross-section of the workpiece material after hard turning. The white appearance of the outermost layer in Fig. 3(a) is a consequence of scattering of white light at the small-sized crystallites (5-500 nm), which are smaller than or comparable to the wavelength of light. Beneath the white layer, there is also a darker structure which is denoted dark layer or over-tempered martensitic layer because of its darker appearance in comparison to the unaffected structure. This layer is often compared to a re-tempered structure since a higher tempering temperature would result in a structure that is easier to etch.

Table 2 provides the experimental results of the morphology of the near surface carbides after hard turning. From the unaffected microstructure the mean carbide diameter was estimated to be 0.34 µm with a standard deviation of 0.18 µm. In general, the carbides had a spherical shape with an aspect ratio (a/b) close to unity. In the investigated samples, B1-B6, no measurable reductions were seen in the carbide diameter as a function of depth below the machined surfaces. The mean carbide diameters within the entire analyzed area (400x20 μm^2) for B1 through B6 are shown in Table 2. Even when comparing the carbide diameter from the first 2 µm below the surface with the carbide diameter from the entire analyzed area, none of the studied samples showed a significant reduction in diameter. Nano-sized carbides were not included in this investigation. The experimental results from the present study are well in agreement with the conclusions made by Chou and Evans [4]; i.e. even though cutting temperatures are high enough to reaustenitize, the holding times (µs) during white layer formation in hard turning are insufficient to dissolve the carbides. As shown in Table 3, comparable results were also obtained when studying the carbide dissolution using DICTRA.

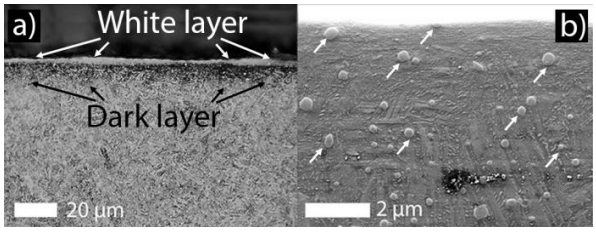

Fig. 3: Cross-sections of the hard turned workpiece material: a) light optical micrograph of the corresponding white and dark layers and b) scanning electron micrograph of the $(Fe,Cr)_3C$ carbides (white arrows).

Using DICTRA, it was observed that the carbide dissolution was suppressed at increased pressures. This is considered to be due to the fact that the two-phase field of austenite and cementite is thermodynamically stable under such conditions as shown in Fig. 4(b-c). Thus, increased pressure during white layer formation in hard turning would not necessarily lead to increased carbide dissolution. When modeling white layer formation in predominantly thermally induced white layers, Ramesh and Melkote [15] calculated the effect of pressure on the A_{c1} temperature for AISI 52100 steel by using the Clausius-Clapeyron equation. The authors found that contact pressures of 1.3 GPa would lower A_{c1} by ~100°C.

Table 2: Carbide mean diameter from the total analyzed depth 20 µm and from the first 2 µm, thicknesses and types of white layers.

Tool condition	**Sample ID**	**Cutting speed [m/min]**	**Carbide mean diameter * [µm]**	**Carbide mean diameter at 2 µm * [µm]**	**White layer thickness [µm]**	**Type of white layer (WL)**
-	Bulk	-	0.34 (0.18)	-	-	-
$V_B \sim 0.04$ mm	B5	30	0.31 (0.14)	0.31 (0.14)	0	-
	B1	110	0.38 (0.18)	0.36 (0.15)	0	-
	B2	260	0.35 (0.17)	0.36 (0.16)	≤ 0.5	Disc. T-WL
$V_B \sim 0.2$ mm	B6	30	0.34 (0.15)	0.32 (0.13)	1.0±0.5	Disc. M-WL
	B3	110	0.34 (0.18)	0.34 (0.17)	1.5±0.5	Cont. T-WL
	B4	260	0.37 (0.19)	0.38 (0.19)	3±1	

* Values in parenthesis are the standard deviations

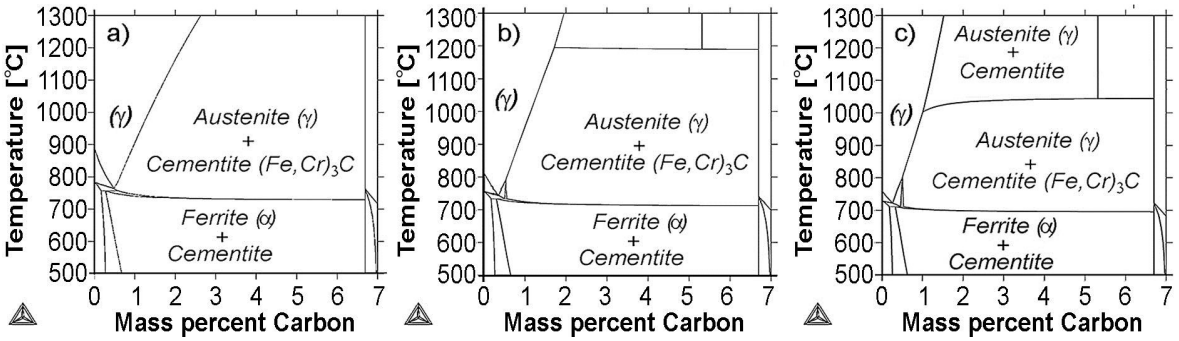

Fig. 4: The effect of pressure on the phase diagram for AISI 52100 steel as calculated using ThermoCalc software (TCFE6). a) p = 1 atm, b) p = 1 GPa and c) p = 2 GPa.

Hence, for predominantly thermally induced white layers, the surface layer will be austenitized at temperatures lower than the conventional A_{c1} (750°C) at atmospheric pressure. Assuming typical hard turning conditions with a holding time of 100 µs at 1000ºC and with heating and cooling rates of $5x10^5$°C/s, the material would be austenitized during 1.1 ms at atmospheric pressure. On the other hand, applying a contact pressure of 1.3 GPa results in a lowering of the A_{c1} temperature and the surface layers would be austenitized during 1.5 ms. Although the increased time due to lowered A_{c1} is considered by using available thermodynamic data (TCFE6) in the DICTRA simulations, the influence of a significantly longer holding time (e.g. 500 µs) was also studied. As can be seen in Table 3, the diametrical changes were comparable to the results obtained after 100 µs holding time. When studying the carbide dissolution kinetics in DICTRA, complete dissolution and re-precipitation as suggested by Barry and Byrne [7] was not likely since the time required for dissolution and re-precipitation would be much longer than the actual process time. However, the effect of strain (plastic deformation) which is known to affect the carbide dissolution kinetics was not included in the simulations. This will be discussed later in this paper.

The DICTRA simulations also made it possible to study the Cr and C profiles from the centre of the carbide through the interface and into the γ-phase. As can be seen in Fig. 5(a-b), the calculated Cr and C profiles after 500 µs at 1000°C and 1 atm show substantial differences both at the interface of the θ/γ as well as inside each phase. In the case of the C profile, there is almost no carbon enrichment at the interface or in the austenite. In the Cr profile however, substantial Cr enrichment is observed at the interface, both inside the carbide as well as in the austenite. Comparable C and Cr profiles were also observed by Zhao et al. [16], who investigated the dissolution of (Fe, $Cr)_3C$ carbides in a Fe-Cr-C system at 860°C by solving a vector-based Stefan-problem with finite γ-cells. From the simulation results the authors observed that the C diffusion occurred rapidly resulting in a flat C profile, while Cr diffusion (substitutional element) was significantly slower and thus resulted in an inhomogeneous Cr profile in the γ-phase. With respect to the carbide dissolution kinetics in a Fe-Cr-C system, Ågren and Vassilev [10] summarized that the dissolution consisted of three stages: i) C diffusion in the γ-phase, ii) Cr diffusion in the carbide to the interface and iii) Cr diffusion into the γ-phase.

Table 3: DICTRA carbide dissolution results at two different conditions.

DICTRA cond.; T = 1000°C, p = 1 atm			
Carbides	**Start diam. [µm]**	**Carbide diameter after:**	
		100 µs	**500 µs**
A	500	499.0	498.8
B	250	249.3	249.1
C	200	199.4	199.2
DICTRA cond.; T = 1000°C, p = 1 GPa			
Carbides	**Start diam. [µm]**	**Carbide diameter after:**	
		100 µs	**500 µs**
A	500	499.23	498.97
B	250	249.46	249.24
C	200	199.52	199.32

The dissolution kinetics of (Fe, $Cr)_3C$ carbides in austenite for a Fe-Cr-C alloy at 910°C were also studied by Liu et al. [17], both theoretically and experimentally by using DICTRA and analytical electron microscopy (AEM). At a temperature of 910°C, the initial stage was completed within less than a second while the two later stages required hours to completion. The experimental results showed that the adjacent austenitic matrix was enriched in Cr during the dissolution process which was in good agreement with the local equilibrium hypothesis. Moreover, in agreement with Ågren and Vassilev [10], also Liu et al. [17] stated that during the initial stage of the carbide dissolution, the reaction was controlled by C diffusion and in a second step by Cr diffusion.

Based on the DICTRA results from the present study on the dissolution kinetics of the (Fe, $Cr)_3C$ carbides, it can be concluded that dissolution and re-precipitation of carbides would not be possible during white layer formation in hard turning involving short holding times (<500 µs) at ~1000°C. Since only a negligible reduction in carbide diameter was observed at 1000°C, the temperature was increased up to 1300°C in incremental steps of 100°C. The simulations showed that temperatures as high as 1300°C must be reached to be able to reduce the diameter of the carbides to an extent that is measurable at such short contact times. In Fig. 6, the diametrical reduction of carbide A as a function of time is shown, where the carbide diameter reduction was ~20 nm after 500 µs. Thus, it can be summarized that even at temperatures as high as 1300°C, complete (Fe, $Cr)_3C$ carbide dissolution is not possible.

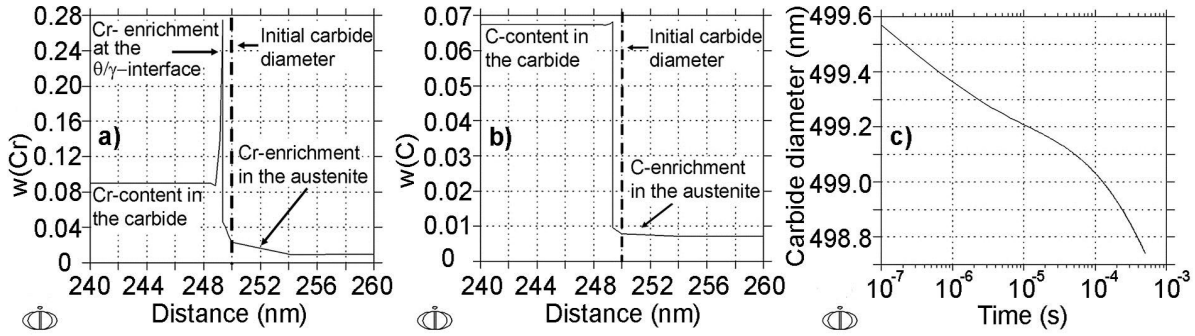

Fig. 5: Simulated a) chromium and b) carbon concentrations as function of the distance from the center of the carbide into the adjacent austenite region. c) The carbide diameter reduction as a function of time. T = 1000°C and p = 1 atm.

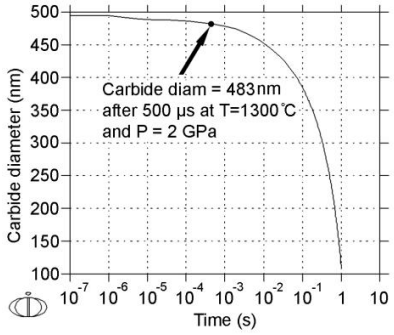

Fig. 6: Change of the diameter as a function of time for carbide A.

As mentioned above, the effect of strain (plastic deformation) was not included in the DICTRA simulations although it is well known that plastic deformation will contribute to dissolve the precipitates. For example, when studying white layers formed on a rail head, Newcomb and Stobbs [18] proposed an alternative mechanism for white layer formation by carbide dissolution. The mechanism was based on the work by Kalish and Cohen [19] in developing models for the strain tempering of martensite. The authors estimated that a dislocation density of $2x10^{13}$ cm^{-2} would be sufficient to dissolve the carbides in a ferritic structure containing 0.6 wt.% C. Thus, by assuming that comparable dislocation densities were created in the rail head due to the shear stresses induced by the wheel, Newcomb and Stobbs [18] suggested that the carbide dissolution took place through the large number of dislocations saturated in carbon transferred from the carbides. In the present study, there was good agreement between the experimental results and the simulations. Therefore, the effect of strain on the carbide dissolution was considered to be limited. However, in spite of a limited effect from the strain on the carbide dissolution, elongated carbides were found near the machined surfaces in all samples containing white layers. As shown in Fig. 7, a large number of elongated carbides are located below the hard turned surface. This occurred irrespective of whether the white layer formation had been predominantly thermally or mechanically initiated. From the microstructure investigation a large number of carbides below the machined surfaces were found to have an aspect ratio (a/b) between 2 and 4.5. This can be compared to an aspect ratio of ~1.05 for the majority of the carbides in the unaffected structure. Relative amounts of elongated carbides in the first 10 µm are shown in Fig. 8 for all of the investigated surfaces. For both of the samples machined with 30 m/min, B5 and B6,) a large number of deformed carbides were found in the outermost surface zone (down to 2 µm). The highest amount was found for the sample hard turned with a worn cutting tool (B6) for which the volume fraction of the deformed carbides at the surface was ~12% compared to ~7% for the surface machined with a fresh tool (B5). For samples machined with the higher cutting speeds, 110 and 260 m/min, an increased volume fraction of deformed carbides was only found when worn cutting tools had been used. In this case volume fractions up to ~8% were observed. The different responses concerning plastic deformation of carbides is considered to be related to the different duration of contact between the work materials and the cutting tools. These results show that the severe plastic deformation that takes place during hard turning is concentrated to the outermost (<2 µm) part of the surface.

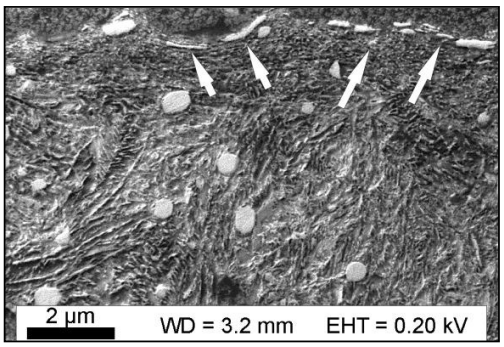

Fig. 7: Scanning electron micrograph of elongated carbides (white arrows) in the M-WL formed during hard turning at 30 m/min utilizing a worn tool.

Generally, due to the high hardness of ~1200 $HV_{0.05}$ at room temperature [20], the iron-chromium carbides (M_3C), are often assumed to fracture rather than to plastically deform. However, attention has to be drawn to the fact that temperature plays an important role in whether the carbides will be plastically deformed or fractured. Keh [21] studied defect structures in cementite particles and how the density of defects increased within the particles during plastic

deformation of 1095 steel. He observed that when the steel was severely deformed at room temperature, most of the plastic flow took place in the ferritic matrix. In contrast, when the same material was deformed at 700°C, gross deformation of the cementite was found even with light optical microscopy, where some of the spherodized particles in the 1095 steel were elongated with aspect ratios (a/b) up to 10.

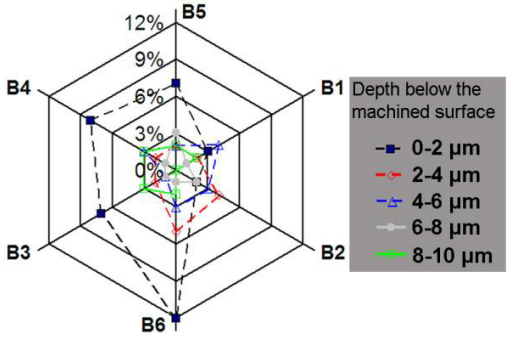

Fig. 8: Polar diagram of the $(Fe, Cr)_3C$ carbides with a/b > 2.

5. Conclusions

In this study the $(Fe, Cr)_3C$ carbide morphology near hard turned surfaces of bainitic hardened AISI 52100 steel was experimentally investigated for both predominantly thermally and mechanically generated white layers. The microstructure results of the mainly thermally induced white layers were also evaluated regarding the dissolution kinetics of the carbides using the DICTRA simulation tool.

The experimental results showed that independent of the type of white layers, no significant reduction in carbide diameter was observed down to 20 µm below the machined surfaces. In agreement with the microstructure investigation, also the analytical results showed negligible carbide dissolution; the diametrical reduction was not more than 2 nm for a carbide with an initial diameter of 500 nm when considering a temperature of ~1000ºC and a duration of contact of 1.5 ms. With respect to the short contact times associated with hard turning, temperatures as high as 1300ºC must be reached to reduce the carbide diameters by measurable values. Therefore, complete dissolution and re-precipitation of $(Fe, Cr)_3C$ carbides in white layers induced during hard turning is not possible.

Down to 4 µm below the machined surface, a large number of carbides showed an elongated appearance (aspect ratio > 2) indicating plastic deformation of the carbides. This shape change was mainly seen within mechanically induced white layers, although it was also found in thermally induced white layers. This paper thus shows that hard turning of AISI 52100 steel may affect the carbide morphology in the near surface region through plastic deformation of the carbides but not through dissolution.

Acknowledgement

The *Area of Advanced Production* at Chalmers University of Technology is acknowledged for their financial support.

References

[1] Klocke F, Brinksmeier E, Wienert K. Capability profile of hard cutting and grinding processes. Ann CIRP 2005:54;2:557-580.

[2] Grzesik W. Advanced Machining Process of Metallic Materials – Theory, Modeling and Application. Oxford Elsevier, 2008.

[3] Bartarya G, Choudhury S K. State of the art in the hard turning. Int J Mach Tool Manu 2012:54:1-14.

[4] Chou YK, Evans CJ. White Layers and Thermal modeling of hard turned surfaces. Int J Mach Tool Manu 1999:39:1863-1881.

[5] Akcan S, Shah S, Moylan SP, Chhabra PN, Chandrasekar S, Yang HTY. Formation of White Layers in Steels by Machining and Their Characteristics. Metall Mater Trans A 2002:33A:1245–1254.

[6] Zurecki Z, Ghosh R, Frey JH. Investigation of White Layers Formed in Conventional and Cryogenic Hard Turning of Steels. Proceedings of IMEC'03, ASME International Mechanical Engineering Congress and Exposition Washington, D.C. November 16-21, 2003:16-21.

[7] Barry J, Byrne G. TEM study on the surface white layer in two turned hardened steels. Mater Sci Eng 2002:A325:356-364.

[8] Hosseini SB, Ryttberg K, Kaminski J, Klement U. Characterization of the Surface Integrity Induced by Hard Turning of Bainitic and Martensitic AISI 52100 Steel. 5th CIRP Conference on High Performance Cutting, Procedia CIRP 2012:1:494–499.

[9] Borgenstam A, Engström A, Höglund L, Ågren J, DICTRA, A Tool for Simulation of Diffusional Transformations in Alloys. J Phase Equilibria 2000:21;3:269-280.

[10] Ågren J, Vassilev GP. Computer Simulations of Cementite Dissolution in Austenite. Mater Sci Eng 1984:64:95-103.

[11] Ågren J. Computer Simulations of Diffusional Reactions in Complex Steels. ISIJ International 1992:32;3:291-296.

[12] Dahlgren R. Prediction of near surface M_3C-carbides after hard turning SAE 52100 Steel. Master Thesis, Chalmers University of Technology, Gothenburg, Sweden, 2012.

[13] Hosseini SB. Beno T. Klement U. Kaminski J. Ryttberg K. Cutting temperatures during hard turning - Measurements and effects on white layer formation in AISI 52100. Journal of Materials Processing Technology. 2014:214; 6:1293-1300.

[14] Beswick JM. The effect of Chromium in High Carbon Bearing Steels. Metallurgical Tranactions A 1987:18A:1897-1906.

[15] Ramesh A, Melkote SN. Modeling of white layer formation under thermally dominant conditions in orthogonal machining of hardened AISI 52100 steel. Int J Mach Tools Manuf 2008: 48: 402–414.

[16] Zhao L, Vermolen FJ, Wauthier A, Sietsma J, Cementite Dissolution at 860 °C in an Fe-Cr-C Steel. Metall Mater Trans A 2005:37A:1841–1850.

[17] Liu ZK, Höglund L, Jönsson B, Ågren J. An Experimtenal and Theoretical Study of Cementite Dissolution in an Fe-Cr-C Alloy. Metallurgical Tranactions A 1991:22A:1745-1752.

[18] Newcomb SB, Stobbs WM. A Transmission Electron Microscopy Study of the White-etching Layer on a Rail Head. Mater Sci Eng 1984:66:195-204.

[19] Kalish D, Cohen M. Structural Changes and Strengthening in the Strain Tempering of Martensite. Mater Sci Eng 1970:6:156-166.

[20] Kagawa A, Okamoto T, Saito K. Hot Hardness of $(Fe, Cr)_3C$ and $(Fe, Cr)_7C_3$ Carbides. Journal of Materials Science 1981:19;8:2546-2554.

[21] Keh A S. Imperfections and plastic deformation of cementite in steel. Acta Metallurgica 1963;11:1101-1103.